

Inherent Relationship between Mechanical Properties and Microstructure of Eutectic Alloy Pb-Cd

Malti Rajput

Assistant Professor, PSPS Government P. G. College for Women Gandhi Nagar Jammu, India

Email: [maltirajput83\[at\]gmail.com](mailto:maltirajput83[at]gmail.com)

Abstract: *The main aesthetics and motivation of the current study was that batch growth of eutectic alloys in fusion would produce high-quality composites with anisotropic properties of greater industrial interest. In the present study conducted for this purpose, the anisotropic hardness of eutectic Pb-Cd alloys was revealed, with particular focus on the relationship between isotropic and anisotropic solidification modes and the microstructure obtained from mechanical properties. Since the essence of composites technology lies in the concept of designing materials with novel properties into acceptable analogues for production, briefly implied in this work is the ability to place strong rigid lamellae in the right place, in the right volume proportions, and in the right orientation.*

Keywords: Eutectic alloys, anisotropic, isotropic, lamellae, composite technology

1. Introduction

One of the most systematic techniques to produce composite materials of Industrial value is anisotropic solidification which includes the periodic growth of eutectic alloys from their molten states. Thermal stability and mechanical properties of composites thus produced are remarkable when compared to their individual constituents. These materials are used at higher service temperatures than their base metal counterparts; and their reinforcement may improve specific stiffness, specific strength, abrasion resistance, creep resistance, thermal conductivity, and dimensional stability. These materials have many advantages than polymer-matrix composites due to their higher operating temperatures, non-flammability, and greater resistance to degradation by organic fluids. Metal-matrix composites are used in automobile industries, drive shafts, extruded stabilizer bars, forged suspension and transmission components, aerospace industries, etc. structural applications include advanced aluminum alloy metal-matrix composites; boron fibers are used as reinforcement for the space shuttle orbiter, and continuous graphite fibers for the Hubble telescope.

2. Experiment Details

The constituent metals Pb (99.97% Thomas Baker Chemicals Limited, m. p.600 K) and Cd (99.99% Alpha Aesar, A Johnson Matthey Company, m. p.594K), were used in the preparation of binary eutectic alloy. The purity of constituent metals was authenticated by thermal analysis as their melting temperatures were found approaching the literature values very closely and is given in the parenthesis. Eutectic alloy Pb-Cd was prepared with weight percent compositional proportions, 64 wt% Pb and 36 wt% Cd. Homogeneity of the eutectic alloy was ascertained by the heat-chill method. The composition of the alloy was confirmed with the determination of its melting temperature by the thermal analysis (LINSEIS STA PT-1000). The experimental melting temperature of eutectic alloy Pb-Cd (513.18 K) was found in good agreement with the literature value (513.20 K)

The technique adopted to compute modulus of rupture, tensile and compressive strengths for the anisotropic and isotropic mode of solidification of eutectic and the parent materials are presented in the following

Anisotropic growth: Pyrex tubes were used to develop rod-shaped growths of alloys in the molten state. An experimental sealed Pyrex tube containing freshly prepared semi-molten eutectic or metal was fixed in the center of an empty graduated beaker (volume $\sim 10^{-3} \text{m}^3$) placed in an air oven at a temperature 30 K above the melting point of the sample. The molten mass in the tube was nucleated by circulating silicone oil at 21 different intervals in an experimental time interval of 5-45 min in a perforated oil reservoir at a temperature of $\sim 300 \text{K}$. The silicone oil barely touched the bottom of the tube, resulting in an anisotropic growth process along the length of the tube. Several samples of the eutectic alloy and its constituent metals grew anisotropically with different but nearly constant growth rates determined by the circulation of an approximately equal volume of oil during the indicated intervals.

Isotropic growth: Critical-sized nuclei grew almost instantaneously in all directions, holding a Pyrex tube containing a melt 30 K above its freezing point perpendicular to an ice bath maintained at $\sim 273 \text{K}$ growth. Many samples of eutectic alloys and their phases grew immediately.

Mechanical strength: After dimensioning with vernier calipers, the test samples were subjected to tensile testing, burst modulus (flexural strength) and compression on a Rockwell hardness tester.

a) Tensile test: Known dimensional samples of anisotropic or instantaneously grown eutectic or non-eutectic materials were tested by holding them perpendicular to tensometer at both ends. A continuously increasing load was applied until the captured sample or ingot was resisted and ruptured approximately at the center of mass.

- b) Modulus of rupture test: Anisotropic or instantaneous samples of eutectic or non-eutectic materials of known dimensions at this modulus of failure were tested by clamping them longitudinally on the tensometer.
- c) Compressive test: Cubic samples of eutectic or non-eutectic materials grown by any solidification method were gently compressed in a tensometer under continuously increasing loads until additional resistive capacity appeared.

This test was performed visually while observing the tearing process. Although they are traditional in nature, they can also be attributed to macro-scales, especially with regard to engineered products. Specimens exhibiting >15% deviation from the mean results in each test were not included in the mechanical property data

Cross-sectional samples were taken at several locations along the ingot (sample). Samples were cast into resin molds and mechanically polished. The sample was electrochemically polished in 800 ml of absolute ethanol, 140 ml of distilled water and 60 ml of perchloric acid (HClO₄) solution at room temperature for 60 seconds. To elucidate the microstructure, samples were chemically etched in a solution of 1 part glycerol, 1 part acetic acid and 4 parts nitric acid at room temperature for 30 seconds. Through this process, grain boundaries and lamellar structures were identified using microstructure parameters using a scanning electron microscope (Jeol T330). Therefore, many samples were investigated and phase growth patterns were photographed during solidification at various growth rates.

3. Results

The mechanical property data provided in tables 1, 2 and 3 for both moderate anisotropic growth ($\sim 2.95 \times 10^{-7} \text{m}^3 \text{s}^{-1}$) and isotropic growth (zero order) rates of the Pb-Cd eutectic alloy phases indicate that the moderate anisotropic growth of eutectic alloy predominates the instantaneous growth of the specimens, whether pure metal or eutectic mixture. Table 4 records mechanical property data of the eutectic alloy Pb-Cd alloy at variable growth velocity. Figures 1-3 represent the variation of mechanical properties of the eutectic alloy with variable anisotropic growth velocity. Figure 4a is the microstructure of the eutectic alloy phases experienced in an ice bath ($\sim 273\text{K}$). The growth characteristics of the microstructure are such that, at large kinetic undercooling, the lamellae formed are of short size, aggressive, disconnected, crossing each other and showing no lamella-matrix relationship. These crystal habits, in fact, result in from a splitting of the main single lamella into the separate single lamellae or a group of single lamellae, evidentially, leading to an anomalous morphology (Fig.4b). However, the growth habits of eutectic alloy phases can gradually be structured to non-aggressive, attaching and parallel to each other reinforcing the matrix with decreasing kinetic under cooling (Figs.4c&5a). The microstructure (Fig.5c) is an evidence for the movement of lamellar-faults. It is this movement, not the formation of crystal faults, which is the important factor to governing the spacing constancy among lamellae. An entirely distinct lamellar microstructure (Fig.5d) of the eutectic alloy is obtained at the moderate

anisotropic growth rate ($\sim 2.95 \times 10^{-7} \text{m}^3 \text{s}^{-1}$) determined by setting the flow interval of silicone oil at ($\sim 5 \times 10^{-4} \text{m}^3$) for 28 minutes. The process is capable of producing lamellae spacing in the microstructure to attain rod like growth which possesses inherent ability to furnish optimum value of the hardness of the eutectic composite alloy Pb-Cd in the current investigation.

The lamellar microstructure indicates that some of the unfavorably oriented lamellae in the eutectic grains with high configuration energy cropped out perpendicularly to the solid-liquid interface leaving other lamella with orientations close to configuration energy to follow preferred crystallographic morphology wherein they align parallel to each other in an attaching manner. These growth habits of the eutectic alloy phases developing the rod like microstructure (Fig.5d) from the melt, implicitly but inherently, exhibit their relationship with moderate anisotropic growth velocity. Microscopic growth observations indicate that the eutectic phase, usually, the rich one when grows from the binary melt, the vicinal melt regions attains richness in the other phase, the first phase continues its growth as a lamella or whisker till the other phase nucleates at a certain super saturation. This super crescent lamella growing over the lamella of the first phase would also continue its growth unless and until another super crescent lamella of the first eutectic phase nucleates as lamella on it. In this manner, the super crescent lamella growth of the eutectic alloy Pb-Cd from the melt produces complete microstructure. The growth front contacting solid liquid interface structure inside the experimental tube and the rising level of the silicone oil along the outer wall of the Pyrex tube rise up nearly with the same pace in the single phase, effectively, decreasing the kinetic under cooling which balances the under cooling due to composition, and originating lamellae length (Figs.4, b&c). By virtue of the growth process, it is possible to obtain long lamellae with damage free surfaces (Fig.5c), which are embedded parallel to each other in an attaching and non aggressive unidirectional lamina (Fig.5d). The mathematical model for the rod like growth of the eutectic system has been developed elsewhere. Microscopic view of the cross sectional samples from various locations of the metals Pb and Cd indicated their growth as lamellar cells where each cell crystallized either from the bulk of the melt or through secondary nucleation.

Computation of Mechanical Property Data:

The hardness of the eutectic alloy has been computed in terms of the following mechanical properties using their respective relations mentioned in the literature:

- (i) Tensile Strength, $T_{\text{rup}} = P/\pi r^2$ -----(1)
- (ii) Modulus of Rupture, $Y_{\text{rup}} = PL/\pi r^3$ -----(2)
- (iii) Compressive Strength, $\sigma_{\text{rup}} = P/\pi r^2$ ----- (3)

In these relations, P is the applied load in Kilograms, L and r respectively are the span and radius of the specimen in meters. The parameters P and r vary in their magnitudes depending on both the size of the specimen being tested and nature of the test.

4. Analysis and Discussion

The analysis of the mechanical property data provided in tables 1, 2 and 3, reveals approximately three fold increase in strength growth observations in each mode of mechanical property of the eutectic composite alloy Pb-Cd at the moderate anisotropic growth rate ($\sim 2.95 \times 10^{-7} \text{m}^3 \text{s}^{-1}$) compared to its instantaneous isotropic (zero order) growth at $\sim 273\text{K}$ and excels its manifold superiority over its parent phases irrespective of mode of the solidification, whether anisotropic or instantaneous. The inferential interpretation of the computed mechanical property data of the eutectic composite alloy Pb-Cd over the entire experimental range of variable growth velocity, presented in table 4, divides the plots in Figs.1-3 into three regions, namely, (i) slow growth region; (ii) moderate growth region and (iii) fast growth region. Among the growth regions, moderate growth region, as is evident from the plots of Figs.1-3, seems to be the most probable one for generating the complete lamellar microstructure of the eutectic alloy (Fig.5d) wherein microstructural parameters, namely, lamella diameter, lamella length, lamella length distribution, volume fraction of lamellae, and the alignment and packing arrangements of lamellae, appear to be nearly obeying the Gauss distribution. The growth ability controlling the microstructural

parameters enables the alloy to attain superiority in mechanical properties in comparison to that of the isotropic growth in an ice bath (Fig.4a) and its constituent phases as well (Tables 1, 2&3) which were found growing as lamellar cells wherein microstructural parameters appear to be consistent with the Weibull distribution (Fig.4).

Table 1: Modulus of rupture* eutectic composite Pb-Cd phases at moderate anisotropic growth ($\sim 2.95 \times 10^{-7} \text{m}^3 \text{s}^{-1}$) and isotropic growth (zero order) rates

Sample	Radius $\text{rx}10^{-3}(\text{m})$	Load P (Kg)	Modulus of rupture $\text{Y}_{\text{rup}} (\text{Mpa})$
Pb-Cd			
Anisotropic growth	4.90	34.30	48.40
Instantaneous isotropic growth	4.90	9.00	12.70
Pb			
Anisotropic growth	5.00	5.30	6.60
Instantaneous isotropic growth	5.00	4.20	5.20
Cd			
Anisotropic growth	4.90	2.40	3.50
Instantaneous isotropic growth	4.90	1.70	2.40

*Averaged values

Table 2: Tensile Strength* of eutectic composite alloy Pb-Cd phases at moderate anisotropic growth ($\sim 2.95 \times 10^{-7} \text{m}^3 \text{s}^{-1}$) and isotropic growth (zero order) rates

Sample	Radius, $\text{rx}10^{-3} (\text{m})$	Load, P (Kg)	Tensile strength $\sigma_{\text{rup}} (\text{MPa})$	Elongation Percentage (%)
Pb-Cd				
Anisotropic growth	2.10	77.20	54.60	7.88
Instantaneous isotropic growth	2.10	20.40	14.40	3.77
Pb				
Anisotropic growth	1.98	10.20	8.10	7.2
Instantaneous isotropic growth	1.98	9.80	7.80	3.45
Cd				
Anisotropic growth	1.89	6.40	5.60	12.1
Instantaneous isotropic growth	1.90	5.20	4.50	8.60

*Averaged values

Table 3: Compressive Strength* of eutectic composite alloy Pb-Cd phases at moderate anisotropic growth ($\sim 2.95 \times 10^{-7} \text{m}^3 \text{s}^{-1}$) and isotropic growth (zero order) rates

Sample	Radius $\text{rx}10^{-3}(\text{m})$	Load P (Kg)	Compressive strength $\sigma_{\text{rup}} (\text{MPa})$
Pb-Cd			
Anisotropic growth	2.01	78.80	61.50
Instantaneous isotropic growth	2.00	20.90	16.30
Pb			
Anisotropic growth	2.01	14.40	11.10
Instantaneous isotropic growth	2.00	12.00	9.30
Cd			
Anisotropic growth	1.88	7.70	6.80
Instantaneous isotropic growth	1.87	6.10	5.40

*Averaged values

Table 4: Mechanical property data* of eutectic composite alloy Pb-Cd at different growth rates

Growth velocity $\text{v} \times 10^{-7} \text{m}^3 \text{s}^{-1}$	Modulus of rupture $\text{Y}_{\text{rup}} (\text{MPa})$	Tensile strength $\text{T}_{\text{rup}} (\text{MPa})$	Compressive strength $\sigma_{\text{rup}} (\text{MPa})$
0.48	13.36	14.00	19.52
0.68	14.47	15.40	20.45

1.05	16.76	17.20	23.43
1.35	20.56	21.99	27.62
1.64	25.17	25.80	32.86
1.96	30.36	31.20	40.96
2.18	36.56	36.60	47.51
2.42	41.06	42.30	54.70
2.63	45.58	49.00	59.56
2.78	47.06	52.90	61.20
2.95	48.40	54.60	61.50
3.13	47.06	54.20	60.42
3.32	45.05	53.00	55.82
3.54	41.65	49.80	48.41
3.75	36.04	44.80	42.15
4.00	31.27	38.10	34.72
4.28	24.71	29.70	30.32
4.46	22.00	25.00	25.43
4.72	17.75	20.00	22.46
5.29	15.82	17.20	20.82
6.95	15.44	15.80	20.46

*Averaged values

The physical significance of the plots of Figs.1-3 to be drawn is that the variation of an anisotropic mechanical property over the entire experimental range of growth

velocity furnishes an evidence of its dependence as linear, optimum and linear respectively in the slow, moderate and fast growth regions of solidification. The physical concept implicitly generates strength-growth relationship, which follows an identical form of the Weibull probability distribution curve, since the microstructural parameters obey the distribution particularly in the slow and fast growth regions (Fig.4). The consequences thereof, the curve has two

cut-off points corresponding to a lower strength limit in the slow and fast growth regions, and an upper strength limit in the moderate growth regions. The latter is equivalent to the theoretical strength of the lamellae, as the microstructural parameters nearly obey Gauss distribution (Fig.5d), in the absence of any internal defects or surface flaws which are responsible for the reduced strength.

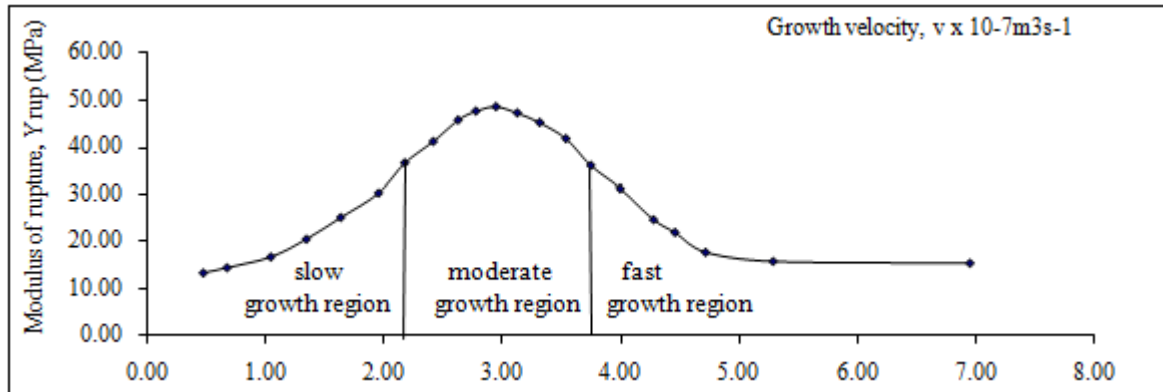


Figure 1

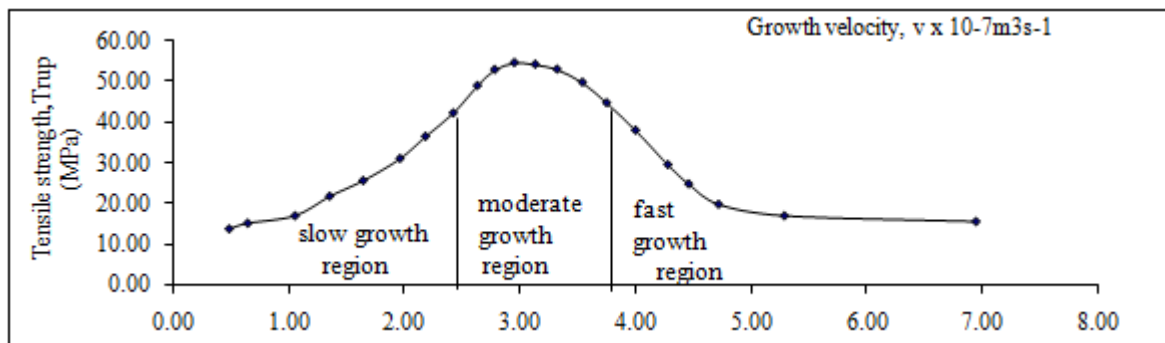


Figure 2

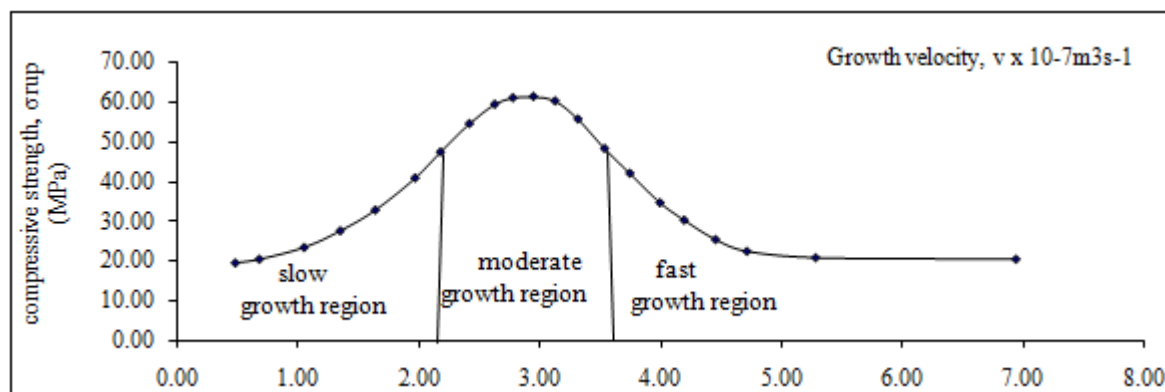


Figure 3

The observed stress enhancement of each mechanical mode of macro hardness of the eutectic composite alloy (Figs.1-3) in the moderate anisotropic growth region is related to the lamellar growth habits of the eutectic phases from the melt (Fig.5). The lamellae are the crystallites practically having no density of dislocations, particularly when they are developed in the moderate growth region. In this region, the lamellar structure themselves parallel to each other in an attaching and non-aggressive unidirectional lamina (Fig.5d) reinforcing the matrix where there is a perfect lamella-matrix bond. Primarily, the lamellar growth of the eutectic

alloy expresses higher strength ability over its instantaneous growth (Fig.4a) and constituent phases (Tables 1, 2&3), since the lamellae of grown eutectic phases are in equilibrium with matrix resulting in an increase in the hardness of the eutectic alloy, while Fig.4 expresses distorted structure of the eutectic alloy in which lamellae appear to be aggressive, non-attaching and irregular thin crystals that produce fragile matrix of the alloy.

The discontinuous change in spacing in the absence of faults (Fig.5c) is the movement of the lamellar-faults, which is an

evidence for the fault mechanism. This implies that it is the movement of the lamellar faults, not the formation of the faults, which is the most important factor in controlling the spacing among lamellae. The lamellar cells of the pure eutectic phases would develop dislocations even with virtue less growth by fault-mechanism from the melt and consequently, offer much lower strength of the alloy. Hardness is actually the structural property of the physical body by virtue of which it resists its permanent deformation. The slight increase in the hardness of the anisotropically solidified eutectic phases (Tables 1, 2&3) in comparison with their instantaneous isotropic growth ($\sim 273\text{K}$) results in from the tendency for linear arrangements of the crystallites although having dislocations. Such growth habits of the pure eutectic phases also develop in the morphology of the eutectic alloy structured obtained by instantaneous isotropic growth from a strength point of view. It is worthwhile to explain the experimental finding that the eutectic alloys with instantaneous growth nearly twice stronger than that of individual constituent metal. The superiority of the alloy over its constituent metals, in fact, is the result of specific modulus and specific strength. The higher specific modulus and specific strength of the alloy means that the weights of constituents can be reduced. This is the factor of great importance in moving constituents where reductions in weight result in a great efficiency of a linear alignment of

the lamellae especially during the eutectic halt, though in the random orientation, yet its elongation (Table 2) to fracture is much lower than constituent metals.

A comparative perusal of the modes of mechanical property (Tables 1, 2, 3&4) further reveals that the compressive mode is slightly higher than the tensile, which in turn showing an edge over the modulus of rupture ($\sigma_{\text{rup}} > T_{\text{rup}} > Y_{\text{rup}}$). In view of the strength mode order, an explanation may be proposed that the phenomenon of binary or multiphase growth from the eutectic melt certainly influences the lamella's length. In the current investigation, two eutectic metal phases would solidify as super crescent lamellae and the length of metal-lamella gets shortened during the growth process. Since the complete lamella is an attachment of two non-aggressive ductile metal lamellae, the efficiency of the lamellae in stiffening and reinforcing the matrix decreases as the lamella length decreases (Fig.5b). Lamella ends play an important role in the fracture of short lamella composites (Fig.5b) and also in continuous lamella composites (Fig.5c), since the long lamellae may break down into discrete lengths

Diversity of morphologies of Pb-Cd eutectic composite alloy at different modes of solidification in the slow and fast growth regions

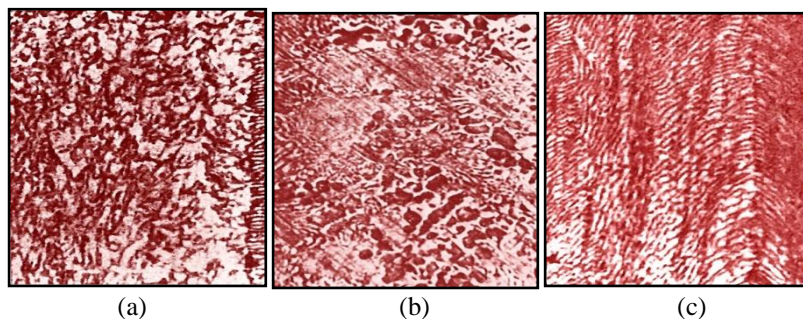


Figure 4: (a) Microstructure in an ice bath at $\sim 273\text{K}$ exhibiting random distribution of crystallites crossing each other showing no crystallite matrix relationship (1800x); (b) Microstructure indicating evolution of lamellae at growth velocity $5.2 \times 10^{-7} \text{m}^3 \text{s}^{-1}$, growth direction from bottom to top (1800x) (c) Microstructure showing the tendency of lamellae for aligning each other at growth velocity $1.96 \times 10^{-7} \text{m}^3 \text{s}^{-1}$, growth direction from bottom to top (1800x).

Diversity of morphologies of Pb-Cd eutectic composite alloy at variable growth rates in the moderate growth region

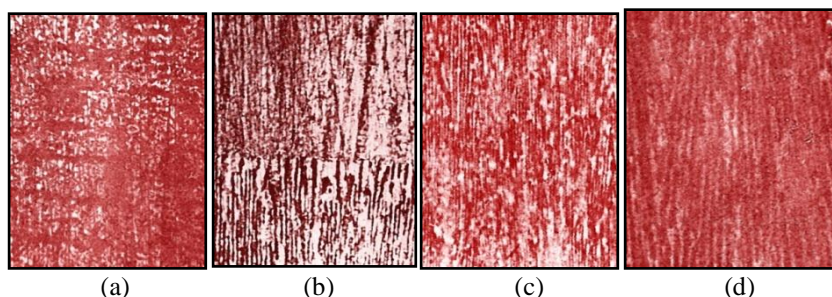


Figure 5: a) Microstructure depicting lamellar tendency of the eutectic phase from melt at growth velocity $3.54 \times 10^{-7} \text{m}^3 \text{s}^{-1}$, growth direction from bottom to top (1800x); (b) Microstructure consisting of short lamellae of eutectic phases at growth velocity $2.63 \times 10^{-7} \text{m}^3 \text{s}^{-1}$, growth direction from bottom to top (1800x); (c) Microstructure governing lamellar faults of long lamellae at growth velocity $2.42 \times 10^{-7} \text{m}^3 \text{s}^{-1}$, growth direction from bottom to top (1800x); (d) Microstructure demonstrating constant spacing among lamellae and projecting rod like growth at moderate growth velocity $2.95 \times 10^{-7} \text{m}^3 \text{s}^{-1}$, growth direction from bottom to top (1800x).

5. Conclusion

The experimental details adopted with the object to reveal the relationship between microstructural parameters resulting-in by isotropic and anisotropic modes of solidification, and mechanical parameters of the eutectic composite alloy Pb-Cd are given in the chapter II. A succinct implicitness in the present approach comprehensively reveals the variation of mechanical properties, namely, tensile strength, modulus of rupture, and compressive strength, over the experimental range of growth velocity. The strength-growth relationship follows an identical form of Weibull distribution curve indicating the obedience of microstructural parameters to the distribution. The curve has two cut-off points which express three regions, namely, slow, moderate and fast growth regions. The slow and fast growth regions correspond to a lower strength limit and moderate growth region correspond to an upper strength limit. The slow and fast growth regions of solidification are found to produce almost comparable results of mechanical properties, while an explanation for the mechanical results of the moderate growth region, being unique, is presented. Moderate anisotropic growth region produces a complete lamellar microstructure of the eutectic alloy, since the microstructural parameters obey Gauss distribution in this region. In this particular structure, the lamellae with damage free surfaces are embedded parallel to each other in an attaching and non-aggressive unidirectional lamina where there is perfect lamella-matrix bond strengthening the eutectic alloy approximately three times of its isotropic growth and manifold superior to its constituent phases irrespective of mode of the growth. Ability evidences of the strength of the eutectic composite alloy Pb-Cd authenticate that the alloy can have optimum hardness at the moderate anisotropic growth velocity ($\sim 2.95 \times 10^{-7} \text{ m}^3 \text{ s}^{-1}$) in the current work.

References

- [1] Agarwal, B. D., Broutman, L. J., & K Chandrashekhara. (2018). *Analysis and performance of fiber composites*. Hoboken, New Jersey Wiley.
- [2] Ashby, M. F., & Jones, D. R. H. (2019). *Engineering materials I: an introduction to properties, applications and design*. Amsterdam: Butterworth-Heinemann.
- [3] Budinski, K. G., & Budinski, M. K. (2005). *Engineering materials: properties and selection*. Upper Saddle River Nj: Pearson Prentice Hall.
- [4] Callister, W. D. (2004). *Materials science and engineering: an introduction*. New York: Wiley.
- [5] Cartledge, H. C. Y., & Baillie, C. A. (1999). Studies of microstructural and mechanical properties of Nylon/Glass composite Part II The effect of microstructures on mechanical and interfacial properties. *Journal of Materials Science*, 34 (20), 5113–5126. <https://doi.org/10.1023/a:1004765201803>
- [6] Cauchi Savona, S., & Hogg, P. J. (2006). Effect of fracture toughness properties on the crushing of flat composite plates. *Composites Science and Technology*, 66 (13), 2317–2328. <https://doi.org/10.1016/j.compscitech.2005.11.038>
- [7] Chandler, H., & Asm International. (1999). *Hardness testing*. Materials Park, Oh: Asm International.
- [8] Charles Ronald Tottle. (1985). *An encyclopaedia of metallurgy and materials*. Estover: Macdonald And Evans.
- [9] Chou, T.-W., McCullough, R. L., & Pipes, R. B. (1986). Composites. *Scientific American*, 255 (4), 192–203. <https://doi.org/10.1038/scientificamerican1086-192>
- [10] Clyne, T. W., & Hull, D. (2019). *An introduction to composite materials*. Cambridge: Cambridge University Press.
- [11] CLYNE, T., MARKAKI, A., & TAN, J. (2005). Mechanical and magnetic properties of metal fibre networks, with and without a polymeric matrix. *Composites Science and Technology*, 65 (15-16), 2492–2499. <https://doi.org/10.1016/j.compscitech.2005.05.037>
- [12] Cortés, D. A., Hogg, P. J., Tanner, K. E., & Ren, G. (2007). Mechanical properties of carbon-fibre reinforced silicate matrix composites. *Materials & Design*, 28 (5), 1547–1554. <https://doi.org/10.1016/j.matdes.2006.02.014>
- [13] Courtney, T. H. (1990). *Mechanical behavior of materials*. New York Etc.: Mcgraw-Hill.
- [14] Dowling, N. E. (2007). *Mechanical behavior of materials: engineering methods for deformation, fracture, and fatigue*. Upper Saddle River, N. J.: Pearson/Prentice Hall.
- [15] Farag, M. M. (2008). *Materials and process selection for engineering design*. Boca Raton: Crc Press.
- [16] Gamstedt, E. K., & Östlund, S. (2001). Fatigue propagation of fibre-bridged cracks in unidirectional polymer-matrix composites. *Applied Composite Materials*, 8 (6), 385–410. <https://doi.org/10.1023/a:1012677604599>
- [17] George Ellwood Dieter. (1988). *Mechanical metallurgy by George E. Dieter*. New York: Mcgraw-Hill.
- [18] Han, P. (1992). *Tensile testing*. Materials Park: Asm International.
- [19] Hollaway, L. (1994). Handbook of Polymer Composites for Engineers. In *The Open Library*. Retrieved from https://openlibrary.org/books/OL12000916M/Handbook_of_Polymer_Composites_for_Engineers
- [20] Hunt, J. D., & Jackson, K. A. (1966). Binary Eutectic Solidification. *Transactions of the Metallurgical Society of AIME*, 236 (6), 843–852.
- [21] Ju, J., Morgan, R. J., Creasy, T. S., & Shin, E. E. (2006). Transverse Cracking of M40J/PMR-II-50 Composites under Thermal—Mechanical Loading. *Journal of Composite Materials*, 41 (9), 1067–1086. <https://doi.org/10.1177/0021998306067260>
- [22] K H G Ashbee. (1993). *Fundamental principles of fiber reinforced composites*. Lancaster: Technomic.
- [23] Knauth, P., & Schoonman, J. (2006). Nanostructured Materials: Selected Synthesis Methods, Properties and Applications. In *Google Books*. Retrieved from https://books.google.com/books?hl=en&lr=&id=TCbrBwAAQBAJ&oi=fnd&pg=PP7&dq=info:gKgFJuadkvoJ:scholar.google.com&ots=HtV29xx5Sw&sig=_2yY7e1nEED3_zH0hQduW-8Cybk

- [24] Krishan Kumar Chawla. (2016). *Composite materials: science and engineering*. New York Springer-Verlag Cop.
- [25] Kuhn, H., Medlin, D., & Asm International. Handbook Committee. (2000). *ASM handbook. Volume 8, Mechanical testing and evaluation*. Materials Park, Oh: Asm International.
- [26] Liang, J.-Z., & Yang, Q.-Q. (2007). Mechanical, Thermal, and Flow Properties of HDPE–Mica Composites. *Journal of Thermoplastic Composite Materials*, 20 (2), 225–236. <https://doi.org/10.1177/08927057074592>
- [27] Mallick, P. K. (1993). *Fiber-reinforced composites: materials, manufacturing, and design*. New York: M. Dekker.
- [28] Pal, R. (2005). Porosity-dependence of Effective Mechanical Properties of Pore-solid Composite Materials. *Journal of Composite Materials*, 39 (13), 1147–1158. <https://doi.org/10.1177/0021998305048744>
- [29] Peters, S. T. (1998). *Handbook of composites*. London: Chapman & Hall.
- [30] Reinhart, T. J., Asm International. Handbook Committee, & Al, E. (1987). *Engineered materials handbook*. Metals Park, Oh: Asm International.
- [31] Sharma, B. L. (2004). Anisotropic lamellae growth and hardness of eutectic composite alloy Pb–Sn. *Journal of Alloys and Compounds*, 385 (1-2), 74–85. <https://doi.org/10.1016/j.jallcom.2004.04.112>
- [32] Strong, A. B., Ploskonka, C. A., Society Of Manufacturing Engineers, & Sme. (1989). *Fundamentals of composites manufacturing: Materials methods, and applications*. Dearborn, Mich.
- [33] Tang, H. C., Nguyen, T., Chuang, T., Chin, J., Lesko, J., & Wu, H. F. (2000). Fatigue Model for Fiber-Reinforced Polymeric Composites. *Journal of Materials in Civil Engineering*, 12 (2), 97–104. [https://doi.org/10.1061/\(asce\)0899-1561\(2000\)12:2\(97\)](https://doi.org/10.1061/(asce)0899-1561(2000)12:2(97))
- [34] Torquato, S. (2005). *Handbook of Materials Modeling* (S. Yip, Ed.). Springer-Verlag, New York (2005).
- [35] Torres, F. G., Arroyo, O. H., & Gomez, C. (2007). Processing and Mechanical Properties of Natural Fiber Reinforced Thermoplastic Starch Biocomposites. *Journal of Thermoplastic Composite Materials*, 20 (2), 207–223. <https://doi.org/10.1177/0892705707073945>

Author Profile



Malti Rajput is working as Assistant Professor in Higher Education Department of Jammu and Kashmir Government since 2010. She is presently posted at PSPS Govt P. G. College for Women Gandhi Nagar Jammu. She has completed her MSc and MPhil from Department of Chemistry, University of Jammu, India